analytical chemistry

Article

pubs.acs.org/ac

Reversible Near-Infrared pH Probes Based on Benzo[*a*]phenoxazine

Wu Liu,[†,∥] Ru Sun,[†,∥] Jian-Feng Ge,*[,†] Yu-Jie Xu,[‡] Ying Xu,[‡] Jian-Mei Lu,*[,†] Isaum Itoh,[§] and Masataka Ihara*[,§]

[†]College of Chemistry, Chemical Engineering and Material Science, [‡]School of Radiation Medicine and Protection, Soochow University, 199 Ren'Ai Road, Suzhou 215123, People's Republic of China

[§]Drug Discovery Science Research Centre, Hoshi University, 2-4-41 Ebara, Shinagawa-ku, Tokyo 142-8501, Japan

Supporting Information

ABSTRACT: Several benzo[*a*]phenoxazine derivatives containing substituted N-aromatic groups are evaluated for their pH-dependent absorption and emission properties. Among the compounds exhibiting optical responses under near-neutral and subacid pH conditions, benzo[*a*]phenoxazine derivatives with an electron-withdrawing aromatic group attached to nitrogen of the imino group show potential application as near-infrared pH sensors. Three water-soluble pH probes based on benzo[*a*]phenoxazine with different pyridinium structures are designed and synthesized. Their reversible pH-dependent emissions in buffer solution containing 0.1% dimethyl sulfoxide (DMSO) locate in 625−850 nm with the fluorescent enhancement of 8.2−40.1 times, and their calculated pK_a values are 2.7, 5.8, and 7.1, respectively. A composite probe containing the three benzo[*a*]phenoxazines shows a linear pH−emission relationship in the range of pH 1.9−8.0. Real-time detection of intracellular pH using an in vitro assay with HeLa cells is also reported.

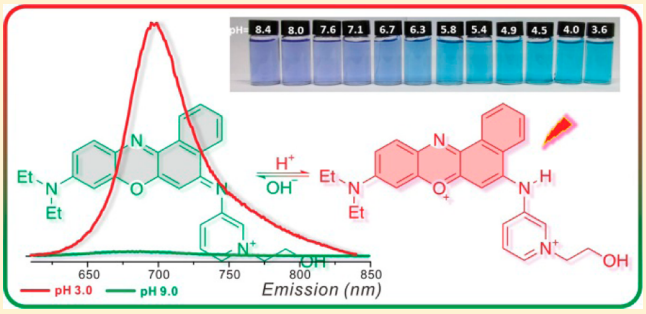

Fluorescent probes that exhibit red and near-infrared (NIR) emission have received considerable attention in the past decade.[1,2] NIR probes that emit in the range of 650−900 nm are especially preferred for sensor design because NIR light can penetrate tissues deeply, minimize damage to biological samples, and decrease the influence of background autofluorescence in tests.[3,4] And intracellular pH plays an important role in organisms since it influences constituents such as cells, enzymes, and proteins, as well as organizational units such as muscles and nervous systems. Although lots of pH indicators have been developed, only some of them present their full emission spectra in the NIR region.[5−8]

The pH probes based on multimethylene cyanine have received attention because of their NIR response,[9−13] but the stability of multimethylene cyanine dyes needs to be improved.[14,15] After an amino-substituted heptamethine cyanine with improved photostability was reported,[16] new NIR probes were developed.[6,7,17−19] The change of fluorescence intensity of these aminocyanine-based probes with pH in aqueous solution is usually less than 7-fold; only one example with a change of up to 15-fold has been reported.[20] Only several NIR pH sensors based on other fluorophores have been reported, for example, BF_2-chelated complexes,[21−23] a styrylcyanine-based probe,[24] diketo-pyrrolo-pyrrole pigments,[25] and an aminoperylene compound.[26] These examples have greatly progressed the theory and application of NIR pH probes. However, new fluorophores for use in NIR pH sensors that are soluble in water, highly sensitive, reversible, and biocompatible are still highly required.

Benzo[*a*]phenoxazine (Scheme 1), a deprotonated structure of benzo[*a*]phenoxazinium, used to be considered an unstable compound because of its imino group. Recent research indicates that benzo[*a*]phenoxazine is a stable, nontoxic compound with excellent bioactivity.[27] Although alkyl-substituted Nile blue derivatives do not show a pH-dependent optical response in near-neutral and subacid pH conditions,[28] a color change of benzo[*a*]phenoxazine with an N-aromatic group has been observed during thin-layer chromatography (TLC) experiments. In this work, five benzo[*a*]phenoxazine derivatives are selected from our bioactive dye library to evaluate their optical response to solution pH.

Scheme 1. Equilibrium between Benzo[*a*]phenoxazine and Benzo[*a*]phenoxazinium

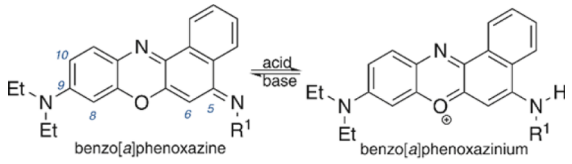

1a: R^1 = (C_6H_4)-OCH_3-*p*;
1b: R^1 = (C_6H_4)-NO_2-*p*.

Received: May 5, 2013
Accepted: July 1, 2013
Published: July 1, 2013

dx.doi.org/10.1021/ac4013539 | *Anal. Chem.* 2013, 85, 7419−7425

EXPERIMENTAL SECTION

Materials. All reagents and solvents (analytical grade) were purchased from TCI Development Co., Ltd. (Tokyo, Japan) or Sinopharm Chemical Reagent Co., Ltd. (Shanghai, China) and used directly. Flash chromatography was performed with silica gel (300−400 mesh). The anion-exchange resin (717 anion-exchange resin) was washed to the nitrate form before use. Hydrochloric acid−citric acid buffer (pH = 0.9), disodium hydrogen phosphate−citric acid buffer (pH = 1.6, 1.9, 2.2, 2.5, 2.7, 3.1, 3.6, 4.0, 4.5, 4.9, 5.4, 5.8, 6.3, 6.7, 7.1, 7.6, 8.0, 8.4, and 9.0), and sodium carbonate−sodium hydrogen carbonate buffer (pH = 9.5) were used.[29] The theoretical pH values of the buffers were used for the buffer solution containing 0.1% or 1.0% dimethyl sulfoxide (DMSO). The pH values of DMSO−H_2O (v/v = 4:1) solutions were adjusted to desired values using aqueous hydrochloric acid (1.0 M) or sodium hydroxide (1.0 M), and their pH values were finally tested by a pH meter. The high K^+ buffer with different pH's for live cell imaging was prepared by the reported method.[30] Compounds **1a** and **1b** and **2a**−**2c** were prepared by a reported method.[27,31]

Apparatus. ^{1}H NMR and ^{13}C NMR spectra were recorded on a Varian 400 MHz spectrometer, and a solvent peak was used as an internal standard. High-resolution mass spectra were recorded on a Finnigan MAT95 mass spectrometer in ESI^+ mode. UV−vis spectra were obtained with a Shimadzu UV-3600 spectrophotometer. Fluorescence emission spectra were measured at room temperature on a Horiba Jobin Yvon FluoroMax-4 fluorescence spectrometer; the excitation and emission slits width are set at 5 nm. Infrared (IR) spectra were recorded on a Nicolet 5200 IR spectrometer using solid samples dispersed in KBr pellets. Melting points were determined on an X-4 microscope electron thermal apparatus (Taike, China). The pH values were measured with a Lei-Ci (pH-3C) digital pH meter (Shanghai, China) using a combined glass−calomel electrode.

Synthesis of Probe 3a. *N,N-Diethyl-5-((1-(2-hydroxyethyl)pyridine-1-ium-2-yl)imino)-5H-benzo[a]phenoxazin-9-amine Nitrate (**3a**).* A mixture of **2a** (394.2 mg, 1.0 mmol) and iodoethanol (0.80 mL, 10.0 mmol) in acetonitrile (50 mL) was heated under reflux for 16 h. The solvent was removed, and the residue was purified by column chromatography on silica gel with gradient elution using methanol/chloroform of 1:15 to 1:5. The crude product was recrystallized from chloroform to obtain the iodide form of **3a**. A methanol solution of the iodide salt was passed through anion-exchange resin (nitrate form). The solvent was evaporated to obtain **3a** as a dark blue power, yield 57%, mp 236−238 °C. IR ν (KBr, cm^{-1}): 3420, 2030, 1630, 1590, 1380, 1110. ^{1}H NMR (400 MHz, DMSO-d_6) δ 8.69 (d, J = 7.9 Hz, 1H, Ar-*H*), 8.65 (d, J = 6.1 Hz, 1H, Ar-*H*), 8.53 (d, J = 7.9 Hz, 1H, Ar-*H*), 8.31 (t, J = 7.6 Hz, 1H, Ar-*H*), 7.91 (t, J = 7.4 Hz, 1H, Ar-*H*), 7.81 (t, J = 7.4 Hz, 1H, Ar-*H*), 7.74 (d, J = 9.1 Hz, 1H, Ar-*H*), 7.63 (d, J = 8.3 Hz, 1H, Ar-*H*), 7.53 (t, J = 6.6 Hz, 1H, Ar-*H*), 7.02 (d, J = 9.1 Hz, 1H, Ar-*H*), 6.70 (s, 1H, Ar-*H*), 6.66 (s, 1H, Ar-*H*), 5.14 (s, 1H, O*H*), 4.56 (br, 2H, CH_2), 3.77 (br, 2H, CH_2), 3.55 (q, J = 6.7 Hz, 4H, 2 × CH_2), 1.18 (t, J = 6.6 Hz, 6H, 2 × CH_3). ^{13}C NMR (101 MHz, DMSO-d_6) δ 161.33, 157.24, 151.77, 150.96, 146.90, 144.86, 144.27, 137.15, 131.65, 131.53, 131.34, 130.04, 129.89, 126.52, 125.58, 123.41, 119.21, 118.77, 112.32, 97.16, 95.70, 58.78, 56.93, 44.84, 12.48. HRMS-ESI^+: m/z = 439.2135 (calcd for $[M - NO_3^-]^+$, 439.2134).

Synthesis of Probe 3b. *N,N-Diethyl-5-((1-(2-hydroxyethyl)pyridine-1-ium-3-yl)imino)-5H-benzo[a]phenoxazin-9-amine Nitrate (**3b**).* Compound **3b** was synthesized by condensing **2b** and iodoethanol using a similar procedure to that described for **3a**. **3b** was obtained as green crystal flakes, yield 65%, mp 232−234 °C. IR ν (KBr, cm^{-1}): 3440, 2030, 1640, 1590, 1380, 1110. ^{1}H NMR (400 MHz, DMSO-d_6) δ 8.74−8.73 (m, 2H, 2 × Ar-*H*), 8.59 (d, J = 7.8 Hz, 1H, Ar-*H*), 8.49 (d, J = 7.7 Hz, 1H, Ar-*H*), 8.20−8.11 (m, 2H, 2 × Ar-*H*), 7.83 (t, J = 7.3 Hz, 1H, Ar-*H*), 7.76 (t, J = 7.3 Hz, 1H, Ar-*H*), 7.60 (d, J = 9.0 Hz, 1H, Ar-*H*), 6.82 (d, J = 8.4 Hz, 1H, Ar-*H*), 6.48 (s, 1H, Ar-*H*), 6.34 (s, 1H, Ar-*H*), 5.31 (s, 1H, O*H*), 4.65 (br, 2H, CH_2), 3.92 (br, 2H, CH_2), 3.48 (q, J = 6.7 Hz, 4H, 2 × CH_2), 1.15 (t, J = 6.3 Hz, 6H, 2 × CH_3). ^{13}C NMR (101 MHz, DMSO-d_6) δ 159.19, 151.08, 150.47, 149.51, 146.26, 139.13, 139.03, 137.40, 137.09, 131.11, 131.04, 130.85, 130.69, 130.02, 128.04, 124.89, 124.42, 123.46, 110.11, 96.71, 95.71, 63.24, 60.14, 44.45, 12.41. HRMS-ESI^+: m/z = 439.2142 (calcd for $[M - NO_3^-]^+$, 439.2134).

Synthesis of Probe 3c. *N,N-Diethyl-5-((1-(2-hydroxyethyl)pyridine-1-ium-4-yl)imino)-5H-benzo[a]phenoxazin-9-amine Nitrate (**3c**).* Compound **3c** was synthesized by condensing **2c** and iodoethanol using a similar procedure to that described for **3a**. **3c** was obtained as green crystal flakes, yield 70%, mp 198−200 °C. IR ν (KBr, cm^{-1}): 3410, 2030, 1630, 1580, 1380, 1130. ^{1}H NMR (400 MHz, DMSO-d_6) δ 8.72 (br, 2H, 2 × Ar-*H*), 8.62 (br, 1H, Ar-*H*), 8.41 (d, J = 7.8 Hz, 1H, Ar-*H*), 7.86 (br, 1H, Ar-*H*), 7.78 (br, 1H, Ar-*H*), 7.64 (br, 1H, Ar-*H*), 7.56 (d, J = 5.2 Hz, 2H, 2 × Ar-*H*), 6.87 (br, 1H, Ar-*H*), 6.56 (s, 1H, Ar-*H*), 6.24 (s, 1H, Ar-*H*), 5.25 (s, 1H, O*H*), 4.50 (br, 2H, CH_2), 3.86 (br, 2H, CH_2), 3.51 (br, 4H, 2 × CH_2), 1.17 (br, 6H, 2 × CH_3). ^{13}C NMR (101 MHz, DMSO-d_6) δ 165.27, 157.76, 150.87, 149.91, 146.45, 145.21, 138.32, 131.24, 131.20, 130.93, 130.24, 129.96, 125.24, 125.04, 123.44, 118.81, 110.79, 96.54, 95.73, 61.29, 60.17, 44.55, 12.42. HRMS-ESI^+: m/z = 439.2140 (calcd for $[M - NO_3^-]^+$, 439.2134).

Preparation of the Test Solutions. Stock solutions (100 μM) of **1a** and **1b** were prepared with DMSO. Each test solution (10 μM) was prepared in a volumetric flask (10 mL) from the corresponding stock solution (1.0 mL) and DMSO−H_2O (v/v = 7:2, 9.0 mL) with different pH's adjusted with aqueous hydrochloric acid or sodium hydroxide to give a total volume of 10 mL. Stock solutions (100 μM) of **3a**−**3c** were prepared in a volumetric flask (100 mL) with DMSO (1.0 mL) and distilled water. Stock solutions (500 μM) of **3a** and **3c** were prepared in a volumetric flask (100 mL) with DMSO (10.0 mL) and distilled water. Each test solution (10 μM) was prepared in a volumetric flask (10 mL) with the corresponding stock solution (1.0 mL, from 100 μM stock solution) and buffer solution to give a total volume of 10.0 mL. The composite solution of probes **3a**−**3c** (27.8 μM) was prepared in a volumetric flask (10 mL) with the composite stock solution (1.0 mL) and the corresponding buffer solution containing 1.0% DMSO, where the composite stock solution is a mixture of **3a** (8.0 mL, from 500 μM stock solution), **3b** (20 mL, from 100 μM stock solution), and **3c** (8.0 mL, from 500 μM stock solution).

Cell Culture and Imaging Methods. HeLa cells were cultured in Roswell Park Memorial Institute culture medium (RPMI-1640) supplemented with 10% calf serum, penicillin (100 U·mL^{-1}), streptomycin (100 μg·mL^{-1}), and L-glutamine (2.5×10^{-4} M) at 37 °C in a 5:95 CO_2−air incubator. Cells with 2×10^5 density were loaded onto a glass-bottomed coverslip with a diameter of 35 mm and cultured for 48 h before use. Fluorescence images of the stained HeLa cells were obtained with a Leica SP2 laser confocal scanning microscope equipped with a 633 nm laser head. Emission was measured for

dx.doi.org/10.1021/ac4013539 | Anal. Chem. 2013, 85, 7419−7425

the range of 650−795 nm. HeLa cells were incubated with the composite probe (0.8 μM, mole ratio of **3a**/**3b**/**3c** = 2:1:2) in PBS buffer (pH = 7.4, 1.03 mL) for 20 min. After removing the nutrient fluid, the high K^+ buffer (pH = 8.0, 1.0 mL) was used to wash the cells, the basic high K^+ buffer (pH = 8.0, 1.0 mL) with nigericin (2 $\mu g \cdot mL^{-1}$) was added, and cells were incubated for 10 min. The system was then changed to acidic high K^+ buffer (pH = 6.0, 1.0 mL) with nigericin (2 $\mu g \cdot mL^{-1}$) and incubated for a further 10 min. The system was finally changed to acidic high K^+ buffer (pH = 4.0, 1.0 mL) with nigericin (2 $\mu g \cdot mL^{-1}$) and incubated for a further 10 min. Treated cells were imaged by fluorescence microscopy. All images were obtained using the same settings and processed with attached software.

RESULTS AND DISCUSSION

Optical Responses of Benzo[*a*]phenoxazines with N-Aromatic Group Substituents to pH. The change in the optical properties of **1a** (Scheme 1) with pH was first evaluated in DMSO−H_2O (v/v = 4:1) solution (Figure 1A). The absorption maximum of **1a** changes from 545 nm (pH = 9.1) to 666 nm (pH = 2.5) with an isosbestic point at 590 nm, and a colorimetric change from pink to azure is observed. The intensity of the emission maximum of **1a** is slightly quenched at lower pH. These results indicate that **1a** is a colorimetric pH indicator rather than a fluorescent sensor. When the electron-donating methoxy group in **1a** is replaced by an electron-withdrawing nitro group to form **1b**, both colorimetric and fluorescent responses to pH are observed (Figure 1B). The absorption maximum of **1b** changes from 565 nm (pH = 5.9) to 683 nm (pH = 1.4) with an isosbestic point at 605 nm, and a colorimetric change from lilac to azure is observed. The intensity of the emission maximum enhances by 32-fold from a very weak band at 641 nm to a more intensive one at 720 nm with increasing hydrion concentration.

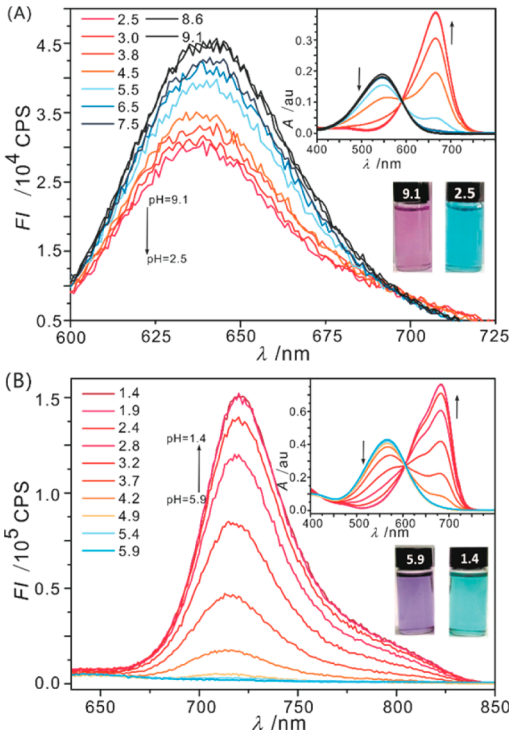

Figure 1. Absorption and emission properties of probes **1a** and **1b** (10 μM) toward different pH values in DMSO−H_2O (v/v = 4:1) solution: (A) probe **1a** (λ_{ex} = 590 nm); (B) probe **1b** (λ_{ex} = 600 nm); insets are the absorption spectra and photographs of the samples.

Protonation of the $\pi-\pi$ conjugated benzo[*a*]phenoxazine to form benzo[*a*]phenoxazinium causes the absorption maximum to exhibit a red shift up to 121 nm (Figure 2). The N-aromatic substituent allowed an equilibrium between benzo[*a*]-phenoxazine and benzo[*a*]phenoxazinium to form in near-neutral or subacid pH conditions. The 5,9-nitrogen atoms serve as electron donors to the benzo[*a*]phenoxazinium moiety of **1a** + H^+, and the weak emission from benzo[*a*]phenoxazinium is induced by intramolecular charge transfer (ICT). The situation is changed when the electron-donating methoxy group in **1a** + H^+ is replaced by an electron-withdrawing nitro group in **1b** + H^+; specific emission is observed when ICT is weakened by the electron-withdrawing inductive effect of the nitro group. Thus, the introduction of electron-withdrawing groups is required to design fluorescent pH probes. The poor solubility of probe **1b** in water will limit the in vitro application, and then the design of water-soluble probes with electron-deficient aromatic groups in an attempt to produce NIR pH probes is prompted in the next stage.

Synthesis and pH-Induced Optical Responses of *N*-Pyridiniumylbenzo[*a*]phenoxazines. *N*-Pyridiniumylbenzo-[*a*]phenoxazines (**3a**−**3c**) were selected to fit the above requirements by alkylation reaction from their pyridinyl derivatives (**2a**−**2c**, Scheme 2). Compounds **2a**−**2c** were heated under reflux overnight with excess iodoethanol to afford the corresponding salts. Nitrate salts were obtained by ion exchange using anion-exchange resin to improve their biocompatibility. Probes **3a**−**3c** are soluble in water, and the imino group serves as the sensitive point to hydrions. The same reaction with iodoethanol was performed using **1a** and **1b**, and no new products were detected by TLC. This indicates the

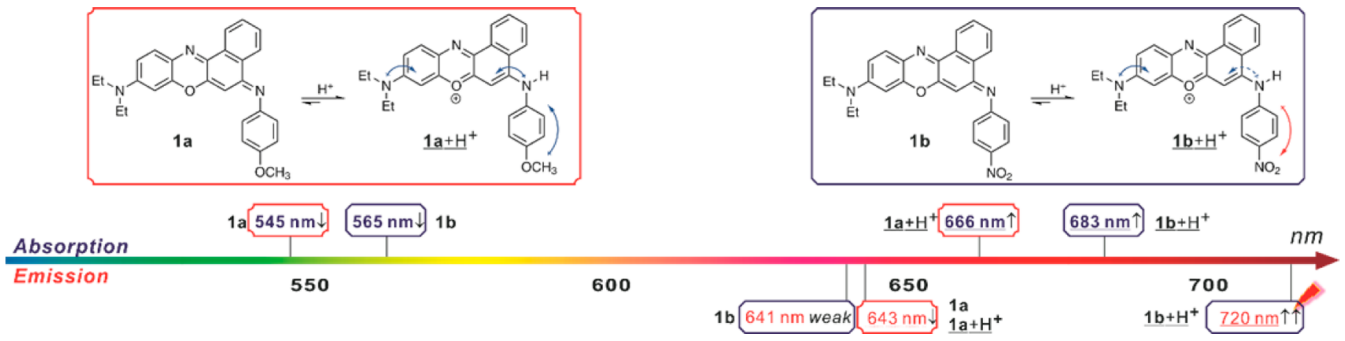

Figure 2. Proposed mechanism and summary of the optical properties of probes **1a** and **1b**.

dx.doi.org/10.1021/ac4013539 | *Anal. Chem.* 2013, 85, 7419−7425

Scheme 2. Synthesis of the Benzo[*a*]phenoxazine-Based Probes (3a−3c)

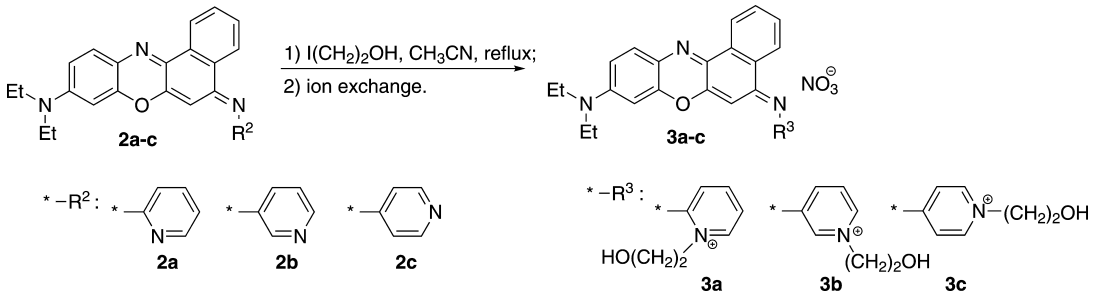

nitrogen atom in the pyridine ring is the only site reactive toward iodoethanol in the starting material.

The absorption maximum of **3a** in buffer solution containing 0.1% DMSO at 630 nm (pH = 6.3, ε = 3.3 × 10^4 $M^{-1}\cdot cm^{-1}$) shifts to 597 nm (pH = 0.9, ε = 2.9 × 10^4 $M^{-1}\cdot cm^{-1}$) (Supporting Information Figure S1A). The weak emission maximum at 723 nm (pH = 6.3) slowly shifts to 688 nm (pH = 0.9), and the full range of emission is in 625−850 nm (Figure 3A). The relative fluorescent intensity of **3a** increases 17.3 times (Supporting Information Table S1), and the calculated pK_a value is 2.7.[32] Probe **3b** has an optical response in pH range of 3.6−8.4 (Figure 3B, Supporting Information Figure S1B). Its absorption maximum at 575 nm (pH = 8.4, ε = 2.3 × 10^4 $M^{-1}\cdot cm^{-1}$) changes to 663 nm (pH = 3.6, ε = 4.0 × 10^4 $M^{-1}\cdot cm^{-1}$). As shown in Figure 3B, the relative fluorescent intensity of **3b** is enhanced by 40.1-fold (Supporting Information Table S1) from the very weak emission at 694 nm (pH = 8.4) to remarkable emission at 697 nm (pH = 3.6). This behavior suggests that **3b** is nearly an off−on-type probe. Its full range of emission is also located in 625−850 nm, and its pK_a is 5.8. The absorption spectra of **3c** exhibit a small shift from 593 nm (pH = 9.5, ε = 2.0 × 10^4 $M^{-1}\cdot cm^{-1}$) to 599 nm (pH = 4.5, ε = 3.4 × 10^4 $M^{-1}\cdot cm^{-1}$) (Supporting Information Figure S1C). Its weak emission at 729 nm (pH = 9.5) shifts to 694 nm (pH = 4.5) with an emission range of 625−850 nm (Figure 3C), its relative fluorescent intensity increases by 8.2 times (Supporting Information Table S1), and its pK_a is 7.1. The pK_a values of the three probes, 2.7, 5.8, and 7.1 for **3a**, **3b**, and **3c**, respectively, indicate that the distance-dependent electron-withdrawing ability between the imino group and ammonium cation in pyridinium influences the affinity between the imino group and hydrion. Therefore, designable pK_a values could be achieved by changing the electron-withdrawing substituent. The photochemical properties of the three probes in water are shown in Table 1. Because the Stokes shifts of the probes are up to 136 nm, self-absorption will be minimized in test. The fluorescence quantum yields of the probes, which were obtained using Oxazine 1 as a standard sample,[33] are increased by 10, 20, and 5 times for **3a**, **3b**, and **3c**, respectively, after protonation of the free bases.

Probes **3a** and **3c** exhibit weak emission at 723 and 729 nm (Figure 3, parts A and C), respectively. Their emission signals are blue-shifted under acidic conditions. In contrast, the emission from **3b** shows a red shift from 694 to 697 nm (Figure 3B), which is similar to the emission from **1b** at different pH's (Figure 1B). The proposed emission mechanism is shown in Figure 4. The real structure of **3a** contains contributions from two resonance structures (i and ii). Resonance structure ii has the characteristic of benzo[*a*]-phenoxazinium, which contributes to the weak emission at

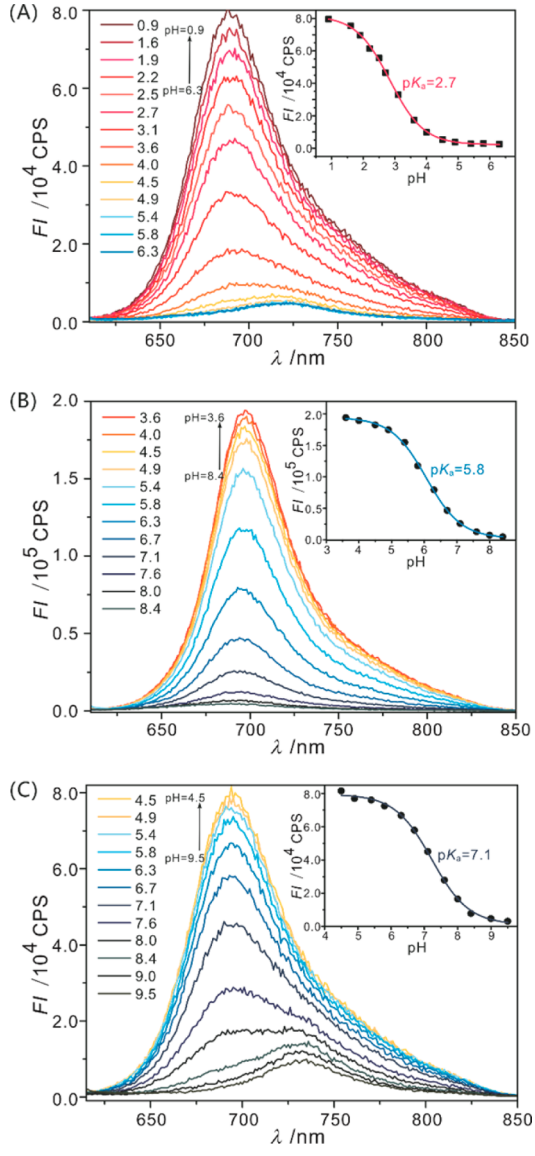

Figure 3. Emission properties of probes **3a**−**3c** (10 μM, λ_{ex} = 600 nm) with different pH values in buffer solution containing 0.1% DMSO: (A) probe **3a**, (B) probe **3b**, (C) probe **3c**; insets are the fluorescence intensity changes with different pH at (A) 688, (B) 697, and (C) 694 nm.

723 nm. The emission properties of **3c** are similar to those of **3a**. Conversely, the real structure of **3b** only involves the benzo[*a*]phenoxazine skeleton, so its absorption and emission properties differ from those of **3a** and **3c**.

Alkyl-substituted Nile blue derivatives tend to aggregate in solution,[34] resulting in new peaks in their concentration-dependent

dx.doi.org/10.1021/ac4013539 | *Anal. Chem.* 2013, 85, 7419−7425

Table 1. Photochemical Properties of Probes 1a, 1b, and 3a−3c

compd	abs_{max} (nm)	em_{max} (nm)	Stokes shift (nm)	extinction coefficient ($M^{-1}\cdot cm^{-1}$)	Φ^a	pK_a
1a (protonated)[b]	666	643	23	3.9×10^4	0.004	4.5[c]
1a (deprotonated)[d]	545	643	98	1.9×10^4	0.01	
1b (protonated)[b]	683	720	37	7.6×10^4	0.005	3.2[e]
1b (deprotonated)[d]	565	641	76	4.3×10^4	0.003	
3a (protonated)[b]	597	688	91	2.9×10^4	0.01	2.7[e]
3a (deprotonated)[f]	630	723	93	3.3×10^4	0.001	
3b (protonated)[b]	663	697	34	4.0×10^4	0.02	5.8[e]
3b (deprotonated)[f]	575	694	119	2.3×10^4	0.001	
3c (protonated)[b]	599	694	95	3.4×10^4	0.01	7.1[e]
3c (deprotonated)[f]	593	729	136	2.0×10^4	0.002	

[a]Oxazine 1 (Φ = 0.14, ethanol) was used as the reference for fluorescence quantum yields in measurements (ref 33). [b]Protonated species were tested in 0.1 M citric acid solution (pH = 1.6) containing 0.1% DMSO. [c]pK_a values were calculated by absorption intensities. [d]Deprotonated species were tested in DMSO. [e]pK_a values were calculated by fluorescence intensities with reported method (ref 32). [f]Deprotonated species were tested in 0.2 M disodium hydrogen phosphate solution (pH = 9.3) containing 0.1% DMSO.

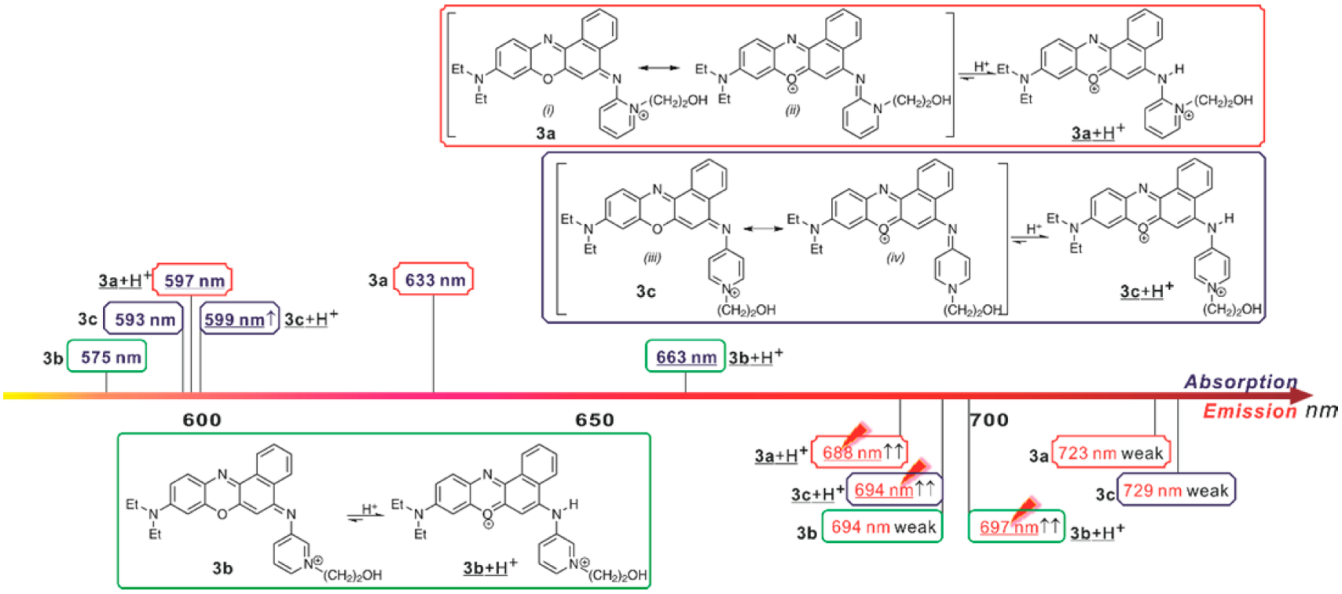

Figure 4. Proposed mechanism and summary of the optical properties of probes **3a−3c**.

normalized absorption spectra. The concentration-dependent optical properties of the *N*-pyridiniumylbenzo[*a*]phenoxazine derivatives were examined. As shown in Supporting Information Figures S2 and S3, the absorption maxima of probes **3a−3c** in acidic or basic conditions showed a linear dependence on concentration (2−20 μM). No obvious new peaks were observed in normalized absorption−concentration plots compared with those reported for alkyl-substituted benzo[*a*]-phenoxazinium. When solutions containing the three probes were changed to low or high pH, the optical properties switched to reflect the new conditions (Figure 5, Supporting Information Figure S4). This indicates that the stable optical properties of these probes make their potential application in real-time quantitative analysis of solution pH.

The probes **3a−3c** have relatively similar structures (Scheme 2), their emission spectra are analogous, and meanwhile the pK_a values are quite different (Figure 3). The hybrid of dyes **3a−3c** would be possible for a NIR composite probe with an extensive pH-sensitive range. After several tries, the composite probe with the mole ratio of **3a**/**3b**/**3c** = 2:1:2 was found to fit the requirement. As shown in Figure 6A, the composite probe with

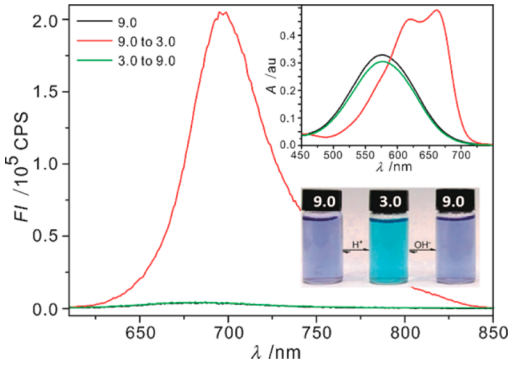

Figure 5. Reversible fluorescence spectra of probes **3b** (10 μM, λ_{ex} = 600 nm) in buffer solution containing 0.1% DMSO; insets are reversible absorption spectra and photograph of the samples.

27.8 μM shows fluorescent response toward wide pH, and the fluorescent intensities are linear agreement with the pH in the range of pH = 1.9−8.0 with R = 99.45%. This makes the quantitative detection of pH achievable through the composite probe.

dx.doi.org/10.1021/ac4013539 | *Anal. Chem.* 2013, 85, 7419−7425

The fluorescent response of the composite probe was also evaluated by fluorescence imaging with HeLa cells (Figure 7). HeLa cells (Figure 7A) were sequentially incubated with the composite probe (0.8 μM) in PBS buffer (pH = 7.4, Figure 7B), basic high K^+ buffer (pH = 8.0, Figure 7C), acidic high K^+ buffer (pH = 6.0, Figure 7D), and then acidic high K^+ buffer (pH = 4.0, Figure 7E). Nigericin (2 $\mu g \cdot mL^{-1}$) was used to promote the acid–base balance between HeLa cells and their conditioned medium.[35] The composite probe shows red emission (Figure 7B) since the acidic condition inside the cancer cell in biological conditions,[36,37] NIR emission was gradually increased (Figure 7C–E) when the concentration of the hydrion was increasing. These in vitro experiments indicate that the composite probe of **3a–3c** can be used to sense pH in vitro.

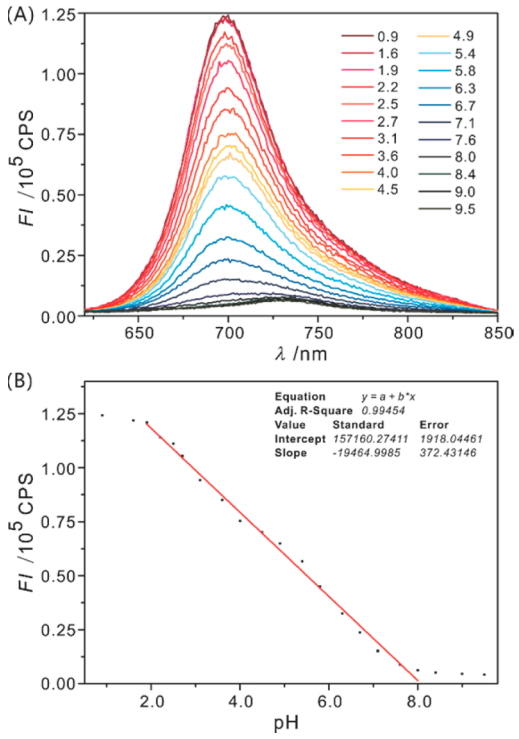

Figure 6. Emission properties of the composite probe by **3a–3c** (27.8 μM, mole ratio of **3a**/**3b**/**3c** = 2:1:2). (A) Emission properties of the composite probe (λ_{ex} = 600 nm) with different pH values in buffer solution containing 1.0% DMSO. (B) The fluorescence intensity changes toward pH at 700 nm.

CONCLUSIONS

The absorption and emission properties of benzo[*a*]-phenoxazine derivatives with an N-aromatic group substituent induced by the equilibrium between benzo[*a*]phenoxazine and benzo[*a*]phenoxazinium were investigated. The compounds exhibited pH-dependent optical responses under near-neutral and subacid conditions. Derivatives with an electron-deficient aromatic group attached to the nitrogen in the imino group of benzo[*a*]phenoxazine showed potential as pH sensors. Three new water-soluble pH probes, **3a–3c**, were designed and synthesized. The emission maxima of **3a–3c** locate at 688, 694, and 697 nm with the full emission ranging from 625 to 850 nm; their optical properties are reversible in aqueous solution containing 0.1% DMSO. The pH-dependent fluorescent intensity of **3b** increased by 40.1 times in aqueous solution, and the pK_a values of **3a–3c** are 2.7, 5.8 and 7.1, respectively. A composite probe, which is mixed by **3a–3c** with the mole ratio at **3a**/**3b**/**3c** = 2:1:2, has a linear pH–emission intensity relationship in pH 1.9–8.0. The in vitro experiment with HeLa cells indicated that the composite probe of **3a–3c** can be used for real-time pH sensing in cells. The reported method could be useful for the design of oxazine-based pH sensors.

ASSOCIATED CONTENT

Supporting Information

Spectra used to characterize **3a–3c**, absorption properties of **3a–3c**, and other related information. This material is available free of charge via the Internet at http://pubs.acs.org.

AUTHOR INFORMATION

Corresponding Author

*E-mail: ge_jianfeng@hotmail.com (J.-F.G); lujm@suda.edu.cn (J.-M.L.); m-ihara@hoshi.ac.jp (M.I.).

Author Contributions

‖W.L. and R.S. contributed equally to this work.

Notes

The authors declare no competing financial interest.

ACKNOWLEDGMENTS

This work was financially supported by the National Natural Science Foundation of China (51273136) and a project funded by the Priority Academic Program Development of Jiangsu Higher Education Institutions. Syntheses were supported by the Creation and Support Program for Start-Ups from Universities, Adaptable and Seamless Technology Transfer Program through Target-Driven R&D, Japan Science Technology Agency (JST).

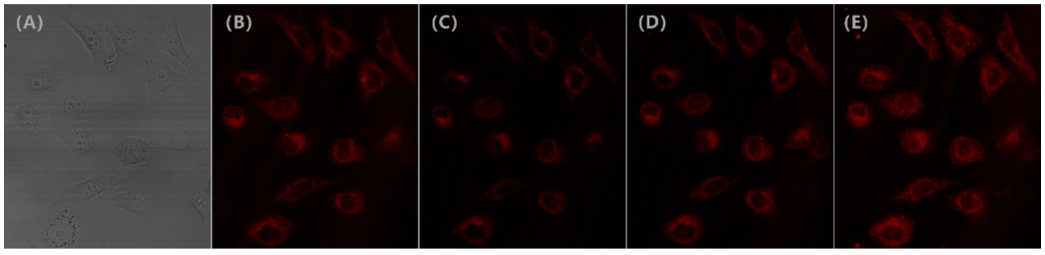

Figure 7. Fluorescence images of HeLa cells with composite probe of **3a–3c** (mole ratio of **3a**/**3b**/**3c** = 2:1:2): (A) bright-field image; (B) fluorescence image of HeLa cells incubated with the composite probe (0.8 μM) in PBS buffer (pH = 7.4) for 20 min; (C) fluorescence image of HeLa cells incubated with high K^+ buffer (pH = 8.0) with nigericin (2 $\mu g \cdot mL^{-1}$) for 10 min; (D) fluorescence image of HeLa cells incubated with high K^+ buffer (pH = 6.0) with nigericin (2 $\mu g \cdot mL^{-1}$) for 10 min; (E) fluorescence image of HeLa cells incubated with high K^+ buffer (pH = 4.0) with nigericin (2 $\mu g \cdot mL^{-1}$) for 10 min.

REFERENCES

(1) Yuan, L.; Lin, W.; Zheng, K.; He, L.; Huang, W. *Chem. Soc. Rev.* **2012**, *42*, 622−661.
(2) Luo, S.; Zhang, E.; Su, Y.; Cheng, T.; Shi, C. *Biomaterials* **2011**, *32*, 7127−7138.
(3) Sun, Y.-Q.; Liu, J.; Lv, X.; Liu, Y.; Zhao, Y.; Guo, W. *Angew. Chem., Int. Ed.* **2012**, *51*, 7634−7636.
(4) Boens, N.; Qin, W.; Baruah, M.; De Borggraeve, W. M.; Filarowski, A.; Smisdom, N.; Ameloot, M.; Crovetto, L.; Talavera, E. M.; Alvarez-Pez, J. M. *Chem.—Eur. J.* **2011**, *17*, 10924−10934.
(5) Han, J.; Burgess, K. *Chem. Rev.* **2010**, *110*, 2709−2728.
(6) Wang, L.; Zhu, X.; Xie, C.; Ding, N.; Weng, X.; Lu, W.; Wei, X.; Li, C. *Chem. Commun.* **2012**, *48*, 11677−11679.
(7) Myochin, T.; Kiyose, K.; Hanaoka, K.; Kojima, H.; Terai, T.; Nagano, T. *J. Am. Chem. Soc.* **2011**, *133*, 3401−3409.
(8) Murtagh, J.; Frimannsson, D. O.; O'Shea, D. F. *Org. Lett.* **2009**, *11*, 5386−5389.
(9) Lee, H.; Akers, W.; Bhushan, K.; Bloch, S.; Sudlow, G.; Tang, R.; Achilefu, S. *Bioconjugate Chem.* **2011**, *22*, 777−784.
(10) Hilderbrand, S. A.; Kelly, K. A.; Niedre, M.; Weissleder, R. *Bioconjugate Chem.* **2008**, *19*, 1635−1639.
(11) Lee, H.; Berezin, M. Y.; Guo, K.; Kao, J.; Achilefu, S. *Org. Lett.* **2009**, *11*, 29−32.
(12) Zhang, Z.; Achilefu, S. *Chem. Commun.* **2005**, 5887−5889.
(13) Hilderbrand, S. A.; Weissleder, R. *Chem. Commun.* **2007**, 2747−2749.
(14) Altman, R. B.; Terry, D. S.; Zhou, Z.; Zheng, Q.; Geggier, P.; Kolster, R. A.; Zhao, Y.; Javitch, J. A.; Warren, J. D.; Blanchard, S. C. *Nat. Methods* **2012**, *9*, 68−71.
(15) Altman, R. B.; Zheng, Q.; Zhou, Z.; Terry, D. S.; Warren, J. D.; Blanchard, S. C. *Nat. Methods* **2012**, *9*, 428−429.
(16) Peng, X.; Song, F.; Lu, E.; Wang, Y.; Zhou, W.; Fan, J.; Gao, Y. *J. Am. Chem. Soc.* **2005**, *127*, 4170−4171.
(17) Kiyose, K.; Aizawa, S.; Sasaki, E.; Kojima, H.; Hanaoka, K.; Terai, T.; Urano, Y.; Nagano, T. *Chem.—Eur. J.* **2009**, *15*, 9191−9200.
(18) Tang, B.; Liu, X.; Xu, K.; Huang, H.; Yang, G.; An, L. *Chem. Commun.* **2007**, 3726−3728.
(19) Zhang, W.; Tang, B.; Liu, X.; Liu, Y.; Xu, K.; Ma, J.; Tong, L.; Yang, G. *Analyst* **2009**, *134*, 367−371.
(20) Tang, B.; Yu, F.; Li, P.; Tong, L.; Duan, X.; Xie, T.; Wang, X. *J. Am. Chem. Soc.* **2009**, *131*, 3016−3023.
(21) Deniz, E.; Isbasar, G. C.; Bozdemir, O. A.; Yildirim, L. T.; Siemiarczuk, A.; Akkaya, E. U. *Org. Lett.* **2008**, *10*, 3401−3403.
(22) McDonnell, S. O.; O'Shea, D. F. *Org. Lett.* **2006**, *8*, 3493−3496.
(23) Hall, M. J.; Allen, L. T.; O'Shea, D. F. *Org. Biomol. Chem.* **2006**, *4*, 776−780.
(24) Fan, L.; Fu, Y. J.; Liu, Q. L.; Lu, D. T.; Dong, C.; Shuang, S. M. *Chem. Commun.* **2012**, *48*, 11202−11204.
(25) Schutting, S.; Borisov, S. M.; Klimant, I. *Anal. Chem.* **2013**, *85*, 3271−3279.
(26) Aigner, D.; Borisov, S. M.; Petritsch, P.; Klimant, I. *Chem. Commun.* **2013**, *49*, 2139−2141.
(27) Ge, J.-F.; Arai, C.; Yang, M.; Bakar, A.; Lu, J.; Ismail, N. S. M.; Wittlin, S.; Kaiser, M.; Brun, R.; Charman, S. A.; Nguyen, T.; Morizzi, J.; Itoh, I.; Ihara, M. *ACS Med. Chem. Lett.* **2010**, *1*, 360−364.
(28) Jose, J.; Ueno, Y.; Burgess, K. *Chem.—Eur. J.* **2009**, *15*, 418−423.
(29) Dawson, R. M. C.; Elliot, D. C.; Elliot, W. H.; Jones, K. M. *Data for Biochemical Research*, 3rd ed.; Oxford Science Publications: Oxford, U.K., 1986.
(30) Han, J.; Loudet, A.; Barhoumi, R.; Burghardt, R. C.; Burgess, K. *J. Am. Chem. Soc.* **2009**, *131*, 1642−1643.
(31) Shi, X.-L.; Ge, J.-F.; Liu, B.-Q.; Kaiser, M.; Wittlin, S.; Brun, R.; Ihara, M. *Bioorg. Med. Chem. Lett.* **2011**, *21*, 5804−5807.
(32) Doria, F.; Nadai, M.; Sattin, G.; Pasotti, L.; Richter, S. N.; Freccero, M. *Org. Biomol. Chem.* **2012**, *10*, 3830−3840.
(33) Rurack, K.; Spieles, M. *Anal. Chem.* **2011**, *83*, 1232−1242.
(34) Alves, C. M. A.; Naik, S.; Coutinho, P. J. G.; Gonçalves, M. S. T. *Tetrahedron* **2009**, *65*, 10441−10452.
(35) Yuan, L.; Lin, W.; Feng, Y. *Org. Biomol. Chem.* **2011**, *9*, 1723−1726.
(36) Cardone, R. A.; Casavola, V.; Reshkin, S. J. *Nat. Rev. Cancer* **2005**, *5*, 786−795.
(37) Ohkuma, S.; Poole, B. *Proc. Natl. Acad. Sci. U.S.A.* **1978**, *75*, 3327−3331.